Transport properties of the Fermi hard-sphere system

Angela Mecca, Alessandro Lovato, Omar Benhar, and Artur Polls

Phys. Rev. C **93**, 035802 — Published 8 March 2016

DOI: 10.1103/PhysRevC.93.035802

Transport properties of the Fermi hard-sphere system

Angela Mecca,[1,2] Alessandro Lovato,[3,4] Omar Benhar,[2,1] and Artur Polls[5]

[1] *Dipartimento di Fisica, "Sapienza" Università di Roma, I-00185 Roma, Italy*
[2] *INFN, Sezione di Roma, I-00185 Roma, Italy*
[3] *Argonne Leadership Computing Facility, Argonne National Laboratory, Argonne, IL 60439, USA*
[4] *Physics Division, Argonne National Laboratory, Argonne, IL-60439, USA*
[5] *Departament d'Estructura i Constituents de la Matèria and Institut de Ciències del Cosmos. E-08028 Barcelona, Spain*

(Dated: February 4, 2016)

The transport properties of neutron star matter play an important role in many astrophysical processes. We report the results of a calculation of the shear viscosity and thermal conductivity coefficients of the hard-sphere fermion system of degeneracy ν=2, that can be regarded as a model of pure neutron matter. Our approach is based on the effective interaction obtained from the formalism of correlated basis functions and the cluster expansion technique. The resulting transport coefficients show a strong sensitivity to the quasiparticle effective mass, reflecting the effect of second order contributions to the self-energy that are not taken into account in nuclear matter studies available in the literature.

PACS numbers: 24.10.Cn, 21.30.Fe

I. INTRODUCTION

The transport properties of nuclear matter are known to be relevant to a variety of astrophysical processes, such as neutron star cooling [1] and the gravitational-wave-driven Chandrasekhar-Friedman-Schutz instability of rapidly rotating stars [2].

Following the seminal papers of Flowers and Itoh [3, 4], several calculations of the thermal conductivity and shear viscosity coefficients of nuclear matter have been carried out using the formalism developed by Abrikosov and Khalatnikov [5] within the conceptual framework of Landau's theory of normal Fermi liquids [6]. In these studies, the nucleon effective masses and the in-medium nucleon-nucleon scattering cross sections—needed for the determination of the transport coefficients within the approach of Ref. [5]—have been obtained using effective nucleon-nucleon interactions derived from either G-matrix perturbation theory [7–9] or the approach based on Correlated Basis Functions (CBF) and the cluster expansion technique [7, 10].

The authors of Refs. [7–10] computed the effective masses within the Hartree-Fock approximation, corresponding to first order of the perturbative expansion in powers of matrix elements of the effective interaction[1]. In Ref. [11], hereafter referred to as I, we have employed the CBF effective interaction approach to analyze the accuracy of this approximation for the fermion hard-sphere system of degeneracy ν=4, corresponding to spin and isospin degrees of freedom. The results reported in I show that the inclusion of the energy-dependent second order contributions to the proper self-energy, while leading to small modifications of the quasiparticle spectrum, strongly affects both magnitude and density dependence of the effective mass. In the Hartee-Fock approximation, the ratio between the effective mass of a quasiparticle on the Fermi surface and the bare mass, $m^\star(k_F)/m$, is consistently less than unity and decreases monotonically with density. The second order result, on the contrary, turns out to be larger than one and monotonically increasing. Although a similar pattern had been already observed in several nuclear matter studies performed within G-matrix [12, 13] and CBF perturbation theory [14], as well as within the Self Consistent Green's Function approach [15], the results of these calculations have not been exploited in analyses of the transport coefficients.

In this article, we report the results of a study of the shear viscosity and thermal conductivity coefficients of the fermion hard-sphere system, carried out taking into account perturbative contributions up to second order in the CBF effective interaction discussed in I. In view of future applications to neutron star matter, the degeneracy of the momentum eigenstates has been set to ν=2.

In Sec. II we recollect the expressions of the transport coefficients obtained from the Landau-Boltzmann kinetic equation, while the derivation of the CBF effective interaction for the fermion hard-sphere system with ν=2—involving additional difficulties with respect to the case ν=4—is described in Sec. III. The calculated effective masses and in-medium scattering probabilities are discussed in Secs. IV and V, respectively, while the shear viscosity and thermal conductivity coefficients obtained from our approach are reported in Sec. VI. Finally, In Sec. VII we summarize our findings and state the conclusions.

[1] The scheme based on G-matrix and the Hartee-Fock approximation is generally referred to as Bruenker-Hartree-Fock approximation.

II. TRANSPORT PROPERTIES OF NORMAL FERMI LIQUIDS

In this work, we follow the approach based on Landau's theory of normal Fermi liquids [6], originally developed by Abrikosov and Khalatnikov [5]. Within this scheme, the shear viscosity and thermal conductivity coefficients—denoted η and κ, respectively—are determined from the momentum and energy fluxes obtained from the kinetic equation for the distribution function

$$\frac{\partial n_{\mathbf{k}}}{\partial t} + \frac{\partial n_{\mathbf{k}}}{\partial \mathbf{r}} \cdot \frac{\partial e_{\mathbf{k}}}{\partial \mathbf{k}} - \frac{\partial n_{\mathbf{k}}}{\partial \mathbf{k}} \cdot \frac{\partial e_{\mathbf{k}}}{\partial \mathbf{r}} = I\left[n_{\mathbf{k}}\right] \ , \tag{1}$$

where $e_{\mathbf{k}}$ denotes the energy of a quasiparticle carrying momentum $\mathbf{k}$, and $I\left[n_{\mathbf{k}}\right]$ is the collision integral, the definition of which involves the in-medium scattering probability W.

In general, the scattering probability depends on the initial and final momenta of the particles participating in the process. In the low-temperature limit, however, the system is strongly degenerate, and only quasiparticles occupying states in the vicinity of the Fermi surface can be involved in interactions. As a consequence, the magnitudes of their momenta can be all set equal to the Fermi momentum, and W reduces to a function of the two angular variables θ and ϕ only. The former is the angle between the initial momenta, whereas the latter is the angle between the planes specified by the initial and final momenta, respectively.

The above procedure leads to the expressions [5]

$$\eta_{AK} = \frac{16}{15}\frac{1}{T^2}\frac{k_F^5}{m^{\star 4}}\ \frac{1}{\langle W\rangle(1-\lambda_\eta)} \ , \tag{2}$$

and

$$\kappa_{AK} = \frac{16}{3}\frac{1}{T}\frac{\pi^2 k_F^3}{m^{\star 4}}\ \frac{1}{\langle W\rangle(3-\lambda_\kappa)} \ , \tag{3}$$

where T is the temperature,

$$\lambda_\eta = \frac{\langle W[1-3\sin^4(\theta/2)\sin^2\phi]\rangle}{\langle W\rangle} \ , \tag{4}$$

$$\lambda_\kappa = \frac{\langle W(1+2\cos\theta)\rangle}{\langle W\rangle} \ , \tag{5}$$

and the angular average of a generic function $\mathcal{W}(\theta,\phi)$ is defined as

$$\langle \mathcal{W}\rangle = \int \frac{d\Omega}{2\pi}\ \frac{\mathcal{W}(\theta,\phi)}{\cos(\theta/2)} \ , \tag{6}$$

with $d\Omega = \sin\theta d\theta d\phi$. Note that, as we are considering a system of identical particles, the angular integration is normalised to 2π.

In the above equations, corresponding to the leading terms of low-temperature expansions, $m^\star$ denotes the quasiparticle effective mass evaluated at momentum such that $|\mathbf{k}| = k_F$. Note that the shear viscosity and thermal conductivity coefficients exhibit different T-dependences.

The quasiparticle lifetime τ can also be written in terms of the angular average of the scattering probability, Eq. (6), according to

$$\tau = \frac{1}{T^2}\ \frac{8\pi^4}{m^{\star 3}}\ \frac{1}{\langle W\rangle} \ . \tag{7}$$

Corrections to the Abrikosov-Khalatnikov results were derived by Brooker and Sykes in the late 1980 [16]. Their final results can be cast in the form

$$\eta = \eta_{AK}\frac{1-\lambda_\eta}{4} \times \sum_{k=0}^{\infty}\frac{4k+3}{(k+1)(2k+1)[(k+1)(2k+1)-\lambda_\eta]} \ , \tag{8}$$

and

$$\kappa = \kappa_{AK}\frac{3-\lambda_\kappa}{4} \times \sum_{k=0}^{\infty}\frac{4k+5}{(k+1)(2k+3)[(k+1)(2k+3)-\lambda_\kappa]} \ . \tag{9}$$

The effect of the corrections, measured by the ratio between the results of Ref. [16] and those of Ref. [5], while being moderate on viscosity, turns out to be large on thermal conductivity. One finds $0.750 \le (\eta/\eta_{AK}) \le 0.925$, and $0.417 \le (\kappa/\kappa_{AK}) \le 0.561$.

The above equations show that the input required to obtain η and κ includes the effective masses, the calculation of which has been discussed in I, and the in-medium scattering probability, which can be obtained in Born approximation using the CBF effective interaction.

III. CBF EFFECTIVE INTERACTION

The fermion hard-sphere system is a collection of spin-one-half particles, the dynamics of which are described by the Hamiltonian

$$H = \sum_i \frac{\mathbf{k}_i^2}{2m} + \sum_{j>i} v(r_{ij}) \ , \tag{10}$$

where $\mathbf{k}_i$ is the momentum of the i-th particle, $r_{ij} = |\mathbf{r}_i - \mathbf{r}_j|$ denotes the distance between particles i and j and

$$v(r) = \begin{cases} \infty & , \quad r < a \\ 0 & , \quad r > a \end{cases} \ . \tag{11}$$

By setting the degeneracy of the momentum eigenstates to ν=2 or 4 this system can be regarded as a model of neutron matter or isospin-symmetric nuclear matter, respectively [17]. It should be kept in mind, however, that this analogy is limited to densities below the solidification point. The analysis of Ref. [18] indicates

that for ν=2 solidification occurs at a density ρ_s such that $\rho_s a^3$=0.23. Moreover, at subnuclear densities nuclear matter is known to undergo transitions to superfluid and/or superconducting phases, which are not allowed by the purely repulsive interaction of Eq. (11). Theoretical studies suggest that neutron matter becomes superfluid at density $\lesssim$0.08 fm^{-3} [19].

The results reported in the following sections have been obtained setting m=1 fm^{-1} and a=1 fm.

A. Definition of the CBF effective interaction

The CBF effective interaction, whose detailed derivation can be found in I, is defined as [10, 20]

$$v_{\rm eff}(r) = \frac{1}{m}\left[\boldsymbol{\nabla} f(r)\right]^2 \ , \tag{12}$$

where the function $f(r)$, describes the correlation structure induced by the potential of Eq. (11). The shape of $f(r)$ is obtained from functional minimization of the expectation value of the Hamiltonian (10) in the *correlated* ground state, defined as

$$|\Psi_0\rangle = \frac{F|\Phi_0\rangle}{\sqrt{\langle\Phi_0|F^\dagger F|\Phi_0\rangle}} \ . \tag{13}$$

In the above equation,

$$F = \prod_{j>i} f(r_{ij}) \ , \tag{14}$$

while the state $|\Phi_0\rangle$, describing the system in the absence of interactions, is represented by a Slater determinant of single particle wave functions, consisting of a plane wave and Pauli spinors associated with the discrete degrees of freedom. For any fixed density ρ, all momentum eigenstates corresponding to $|\mathbf{k}| < k_F$, with $k_F = (6\pi^2\rho/\nu)^{1/3}$, are occupied with unit probability.

Within the two-body cluster approximation (see, e.g., Ref. [21]), this procedure yields an Euler–Lagrange equation, to be solved with the boundary conditions dictated by the properties of the hard-core potential, as well as by the requirement that correlation effects vanish for large separation distances

$$f(r \le a) = 0 \quad , \quad f(r \ge d) = 1 \ . \tag{15}$$

The additional constraint

$$f'(d) = 0 \ , \tag{16}$$

that can be fulfilled introducing a Lagrange multiplier λ, enforces continuity of the logarithmic derivative of the two-particle wave function at $r = d$.

The explicit form of the Euler–Lagrange equation is

$$g''(r) - g(r)\left[\frac{\Phi''(r)}{\Phi(r)} + m\lambda\right] = 0 \ , \tag{17}$$

where

$$g(r) = f(r)\Phi(r) \ , \tag{18}$$

with

$$\Phi(r) \equiv r\sqrt{1 - \frac{1}{\nu}\ell^2(k_F r)} \ . \tag{19}$$

In the above equation, $\ell(x) = 3(\sin x - x\cos x)/x^3$ is the Slater function describing the effects of statistical correlations.

For any given values of density, ρ, and correlation range, d, Eq. (17) can be solved numerically to obtain the correlation function $f(r)$, with the lagrange multiplier λ determined by the requirement that Eq. (16) be satisfied. The correlation range d is treated as a free parameter, to be adjusted in such a way as to have

$$E_0 = \frac{3}{5}\frac{k_F^2}{2m} + \frac{\rho}{2}\int_a^d d^3r\ v_{\rm eff}(r)\left[1 - \frac{1}{\nu}\ell^2(k_F r)\right] \ , \tag{20}$$

where $E_0 = \langle H\rangle/N$ is the ground-state expectation value of the Hamiltonian computed using some advanced and accurate many-body technique, such as the variational Fermi Hyper-Netted Chain (FHNC) approach employed in I for the hard-sphere system of degeneracy ν=4. Note that the quantity appearing on the right hand side of Eq. (20) is the expectation value of the effective Hamiltonian

$$H_{\rm eff} = \sum_i \frac{\mathbf{k}_i^2}{2m} + \sum_{j>i} v_{\rm eff}(r_{ij}) \ , \tag{21}$$

in the Fermi gas ground state.

From Eqs. (17)- (19) it clearly appears that $f(r)$ depends explicitly on the degeneracy of the system, ν, through the coefficient of the squared Slater function. The lower the degeneracy of the system, the larger the effect of these correlations, the range of which monotonically increases as the density decreases. As a consequence, in the low-density region the determination of $f(r)$ from the numerical solution of Eq. (17) with ν=2 turns out to be hindered by the presence of long-range statistical correlations, whose effect is significantly larger than in the case ν=4.

Owing to the above difficulty, at $c = k_F a < 0.5$, the value of E_0 obtained within the FHNC approach does not develop a clear minimum as a function of the correlation range, which in this case plays the role of variational parameter. Therefore, it does not provide an upper bound to the ground-state energy of the system. To overcome this problem, and obtain the accurate estimate of E_0 needed to determine the CBF effective interaction at all densities, we have employed the ground-state expectation values of the Hamiltonian of Eq. (10) obtained from both Variational Monte Carlo (VMC) and Diffusion Monte Carlo (DMC) calculations.

B. Monte Carlo calculation of $\langle H\rangle/N$

Within VMC, the multidimensional integrations involved in the calculation of the expectation value of the Hamiltonian in the correlated ground state are performed using Metropolis Monte Carlo quadrature [22]. The trial wave function, chosen to be the same as in the FHNC calculation, is defined as

$$\Psi_T(\mathbf{R}) = \langle \mathbf{R}|\Psi_0\rangle \ , \tag{22}$$

where $|\Psi_0\rangle$ is given by Eq. (13), $\mathbf{R} \equiv \{\mathbf{r}_1, \ldots, \mathbf{r}_N\}$ denotes the set of coordinates specifying the system in configuration space, and $|\mathbf{R}\rangle$ is the corresponding eigenstate.

The infinite system is modeled by considering a finite number of particles in a box, and imposing periodic boundary conditions. As a consequence, the spectrum of eigenvalues of the momentum $\mathbf{k}$ is discretized. For a cubic box of side L, one finds the familiar result

$$k_i = \frac{2\pi}{L} n_i \quad , \quad i = x, y, z \quad , \quad n_i = 0, \pm 1, \pm 2, \ldots \ . \tag{23}$$

In order for the wave function to describe a system with vanishing total momentum and angular momentum, all shells corresponding to momenta such that $|\mathbf{k}| < k_F$ must be filled. This requirement determines a set of "magic numbers", which are commonly employed in simulations of periodic systems. For example, the VMC—as well as DMC—calculations whose results are reported in this article have been performed with 132 particles, corresponding to 66 and 33 momentum eigenstates for degeneracy ν=2 and 4, respectively.

The expectation value of the Hamiltonian in the state described by the trial wave function of Eq. (22) can be cast in the form

$$\langle \Psi_T|H|\Psi_T\rangle = \int d\mathbf{R} \ E_L(\mathbf{R}) P(\mathbf{R}) \ , \tag{24}$$

where the local energy $E_L(\mathbf{R})$ is defined as

$$E_L(\mathbf{R}) = \frac{H\Psi_T(\mathbf{R})}{\Psi_T(\mathbf{R})} \ , \tag{25}$$

and we have introduced the probability density $P(\mathbf{R}) \equiv \Psi_T^*(\mathbf{R})\Psi_T(\mathbf{R})$. Within VMC, the above integral is estimated by a sum over the set $\{\mathbf{R}\}$, consisting of N_c configurations sampled from the distribution $P(\mathbf{R})$ using the Metropolis algorithm

$$\langle \Psi_T|H|\Psi_T\rangle \approx \frac{1}{N_c} \sum_{\mathbf{R}_i \in \{\mathbf{R}\}} E_L(\mathbf{R}_i) \ . \tag{26}$$

The VMC approach can be seen as an alternative to the cluster expansion technique underlying the FHNC approach, allowing for a stringent test of the approximation implied by the neglect of cluster contributions associated with the so-called elementary diagrams [21].

The main drawback of VMC, obviously shared by FHNC, is that the accuracy of the result entirely depends on the quality of the trial wave function. The DMC method [23, 24] overcomes the limitations of the variational approach by using a projection technique to enhance the true ground-state component of the trial wave function. This result is achieved expanding $|\Psi_T\rangle$ in eigenstates of the Hamiltonian according to

$$|\Psi_T\rangle = \sum_n c_n |n\rangle \quad , \quad H|n\rangle = E_n|n\rangle \ , \tag{27}$$

which implies

$$\lim_{\tau\to\infty} e^{-(H-E_0)\tau}|\Psi_T\rangle = c_0|0\rangle \, , \tag{28}$$

with τ being the imaginary time. Provided $|\Psi_T\rangle$ it is not orthogonal to the true ground state, i.e. for $c_0 \neq 0$, in the limit of large τ the above procedure projects out the exact lowest-energy state.

Because the direct calculation of $\exp[-(H-E_0)\tau]$ involves prohibitive difficulties, the imaginary-time evolution is decomposed into N small imaginary-time steps, and complete sets of position eigenstates are inserted, in such a way that only the calculation of the short-time propagator is required. This procedure yields the expression

$$\begin{aligned} &\langle \mathbf{R}_{N+1}|e^{-(H-E_0)\tau}|\mathbf{R}_1\rangle \\ &= \int d\mathbf{R}_2 \ldots d\mathbf{R}_N \ \langle \mathbf{R}_{N+1}|e^{-(H-E_0)\Delta\tau}|\mathbf{R}_N\rangle \\ &\times \langle \mathbf{R}_N|e^{-(H-E_0)\Delta\tau}|\mathbf{R}_{N-1}\rangle \ldots \langle \mathbf{R}_2|e^{-(H-E_0)\Delta\tau}|\mathbf{R}_1\rangle \ , \end{aligned} \tag{29}$$

where, for the sake of simplicity, the dependence on the discrete degrees of freedom has been omitted. Monte Carlo techniques are used to sample the paths $\mathbf{R}_i$ in the propagation. Note that, although Eq. (29) is only exact in the $\Delta\tau \to 0$ limit, its accuracy can be tested performing several simulations with smaller and smaller time step and extrapolating to zero.

The ground-state energy can be conveniently written in terms of the dimensionless quantity ζ, parametrizing the deviation from the energy of the non interacting system, defined through the equation

$$E_0 = \frac{3}{5}\frac{k_F^2}{2m}(1+\zeta) \ . \tag{30}$$

In Figs. 1 and 2 the results of DMC calculations of ζ are compared to the values obtained from the VMC and FHNC approaches—the latter being only available at $c \geq 0.5$—as well as to the predictions of the low-energy expansions, obtained from [25]

$$\begin{aligned} E_0 = \frac{k_F^2}{2m}\Big[&\frac{3}{5} + \frac{2}{3\pi}c + \frac{4}{35\pi^2}(11 - 2\log 2)\, c^2 \\ &+ 0.230 c^3 \Big] \ , \end{aligned} \tag{31}$$

for ν=2 and

$$E_0 = \frac{k_F^2}{2m}\left[\frac{3}{5} + \frac{2}{\pi}c + \frac{12}{35\pi^2}(11-2\log 2)\,c^2 + 0.780c^3 + \frac{32}{9\pi^3}\left(4\pi - 3\sqrt{3}\right)c^4\log c\right], \quad (32)$$

for ν=4.

It clearly appears that the VMC and FHNC results are very close to one another, thus showing that at $c \geq 0.5$ the FHNC approximation does provide an upper bound to the ground-state energy. The accuracy of the variational result is measured by the difference between the VMC—or, equivalently, FHNC—values of ζ and those obtained from DMC. In the case of degeneracy ν=2, illustrated in Fig. 1, this difference ranges between ∼2% and ∼9% at $0.2 \leq c \leq 1$. Note that a 9% difference in ζ translates in a difference of less that 3% in the ground-state energy E_0. The low-density expansion turns out to be also quite accurate, its predictions being within 5% of the DMC results at $c < 0.5$. Figure 2 shows the results corresponding to $\nu = 4$, which exhibit the same pattern.

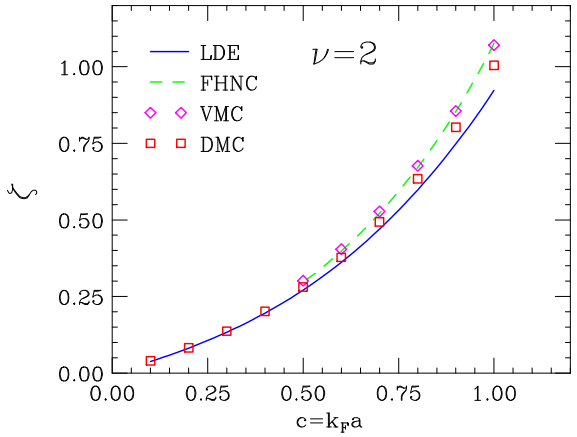

FIG. 1. (color online) c-dependence of the quantity ζ, defined by Eq. (30), for degeneracy ν=2. The solid and dashed lines show the results obtained from the low-density expansion and the variational FHNC approach, respectively. The VMC and DMC results are represented by diamonds and squares. Monte Carlo error bars are not visible on the scale of the figure.

To summarize, the CBF effective interaction of the hard-sphere system with ν=2 has been computed from Eq. (12), choosing the correlation range d in such a way as to reproduce the ground-state expectation value of the Hamiltonian, E_0, obtained using the DMC technique.

IV. QUASIPARTICLE SPECTRUM AND EFFECTIVE MASS

Once the effective interaction has been determined, the calculation of the quasiparticle energy spectrum and effective mass can be performed following the procedure described in I for the case of degeneracy ν=4.

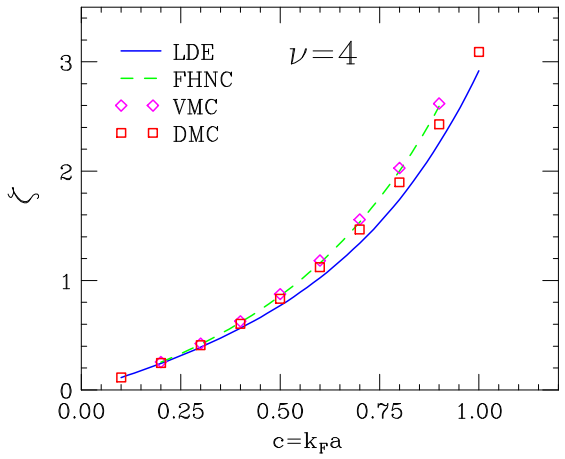

FIG. 2. (color online) Same as in Fig. 1, but for degeneracy ν=4.

The resulting spectrum

$$e(k) = e_0(k) + \mathrm{Re}\;\Sigma[k, e(k)]\;, \quad (33)$$

has been computed including the first and second order contributions to the proper self-energy Σ. The former provides the energy-independent correction corresponding to the Hatree-Fock approximation, while the latter brings about an explicit energy dependence.

The momentum dependence of the quasiparticle energies at c =0.3 and 0.6 is displayed in Fig. 3, while Fig. 4 shows the corresponding effective mass, obtained from

$$m^\star(k) = \left(\frac{1}{k}\frac{de}{dk}\right)^{-1}. \quad (34)$$

Second order corrections to the self-energy have the same effects observed in I for the case $\nu = 4$. The appearance of the energy dependence results in small modifications of the quasiparticle spectrum, but dramatically affects bot the magnitude and the density dependence of the effective mass at $|\mathbf{k}| = k_F$.

For reference, Fig. 4 also shows the effective mass computed using the low-density expansions [26]

$$\frac{m^\star(k_F)}{m} = 1 + \frac{8}{15\pi^2}(7\ln 2 - 1)c^2\;. \quad (35)$$

The difference between the value of $m^\star(k_F)$ evaluated using the CBF effective interaction and the one obtained from Eq. (35) turns out to be $\leq 2\%$ for $c \leq 0.6$, and grows up to 5.5% as the value of c increases up to $c = 1.0$.

V. SCATTERING PROBABILITY

The scattering probability $W(\theta, \phi)$ appearing in the collision integral of Eq. (1) is trivially related to the

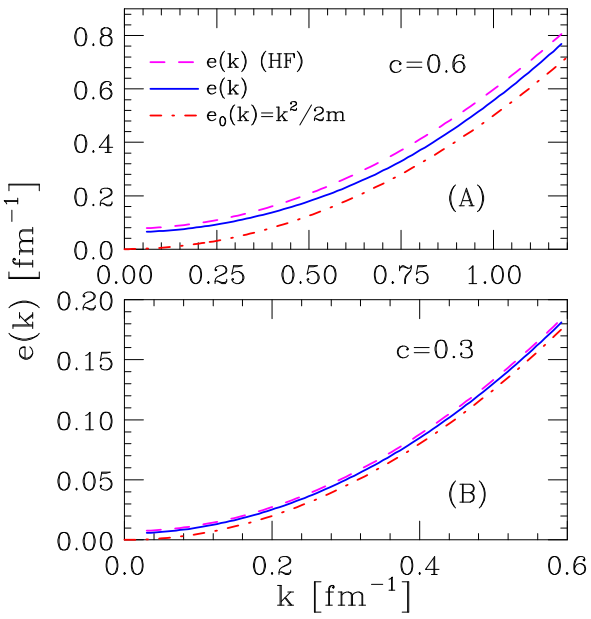

FIG. 3. (color online) Quasiparticle energy of the fermion hard-sphere system of degeneracy ν=2 at $c = 0.3$ [panel (B)] and 0.6 [panel(A)]. The dashed and solid lines correspond to the first order (*i.e.* Hartree-Fock) and second order approximations to the proper self-energy Σ, respectively. For comparison, the dot-dash lines show the kinetic energy spectrum.

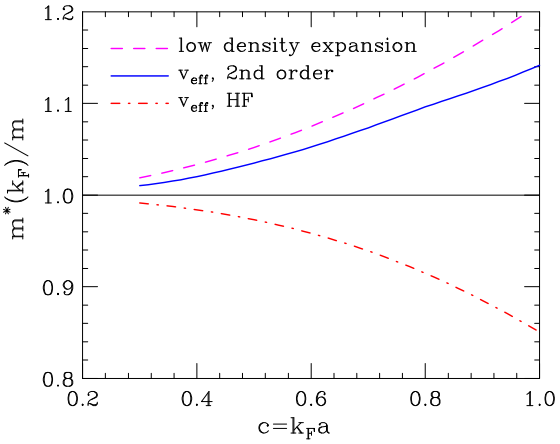

FIG. 4. (color online) c-dependence of the ratio $m^\star(k_F)/m$ for the hard-sphere system of degeneracy ν=2. The dot-dash and solid lines represent the results of calculations carried out using the first and second order approximations to the self-energy. For comparison, the dashed line shows the results computed using the low-density expansion of Eq. (35).

scattering amplitude $f(\theta,\phi)$ through the relation

$$W(\theta,\phi) = \pi \left| \frac{4\pi}{m} f(\theta,\phi) \right|^2 . \tag{36}$$

The scattering amplitude is in turn related to the differential cross section according to

$$\frac{d\sigma}{d\Omega} = |f(\theta,\phi)|^2 . \tag{37}$$

Combining the above equations one finds[2]

$$W(\theta,\phi) = \frac{16\pi^3}{m^2} \left(\frac{d\sigma}{d\Omega} \right) . \tag{38}$$

The scattering cross section is usually expressed in either the laboratory (L) or the center-of-mass (CM) frame. However, the Abrikosov–Khalatnikov formalism is derived in a different frame, referred to as AK frame, in which the Fermi sphere is at rest.

To clarify the connection between AK and CM frames, let us consider the process in which two particles carrying momenta $\mathbf{k}_1$ and $\mathbf{k}_2$ scatter to final states of momenta $\mathbf{k}'_1$ and $\mathbf{k}'_2$. The total energy of the initial state

$$E = \frac{\mathbf{k}_1^2}{2m} + \frac{\mathbf{k}_2^2}{2m} , \tag{39}$$

can be conveniently rewritten in terms of the center of mass and relative momenta, $\mathbf{K} = \mathbf{k}_1 + \mathbf{k}_2$ and $\mathbf{k} = (\mathbf{k}_1 - \mathbf{k}_2)/2$, as

$$E = \frac{\mathbf{K}^2}{2M} + \frac{\mathbf{k}^2}{2\mu} = \mathcal{E} + \mathcal{E}_{\rm rel} , \tag{40}$$

with $M = 2m$ and $\mu = m/2$. In the CM reference frame, in which the center of mass of the system is at rest, $E = E_{\rm cm} = \mathcal{E}_{\rm rel}$, while in the L frame, in which $\mathbf{k}_2 = 0$, $E = E_{\rm L} = 2\mathcal{E}_{\rm rel}$.

In strongly degenerate systems, the magnitude of all momenta playing a role in the determination of the transport coefficients is equal to the Fermi momentum, and conservation of energy requires that the angle between the momenta of the particles participating in the scattering process be the same before and after the collision. In general, however, the angle ϕ between the initial and final relative momenta, $\mathbf{k}$ and $\mathbf{k}' = (\mathbf{k}'_1 - \mathbf{k}'_2)/2$, defined through

$$\cos\phi = \frac{(\mathbf{k}\cdot\mathbf{k}')}{|\mathbf{k}||\mathbf{k}'|} , \tag{41}$$

does not vanish. Hence, for any given Fermi momentum, i.e. for any given matter density, the scattering process in the AK frame is specified by the center of mass energy

$$\mathcal{E}^{\rm AK} = \frac{k_F^2}{2m}(1+\cos\theta) , \tag{42}$$

[2] Note that the relation between scattering probability and cross section reported in Ref. [10], in which the factor $16\pi^3/m^2$ is replaced by $16\pi^2/m^2$, is incorrect.

and the two angles θ and ϕ.

The AK-frame variables can be easily connected to those of the CM reference frame. Since the relative kinetic energy, *i.e.* the energy in the CM reference frame, $E_{\rm c.m.}$, is the same in any frame, we have

$$E_{\rm cm} = \mathcal{E}_{\rm rel}^{AK} = \frac{k_F^2}{2m}(1-\cos\theta) \ , \tag{43}$$

where we have used again the condition that scattering processes involve particles in momentum states close to the Fermi surface. Moreover, the angle between the planes containing ingoing and outgoing momenta, ϕ , is nothing but the angle between the initial and final relative momenta, and can therefore be identified with the scattering angle in the CM frame, setting

$$\Theta_{\rm cm} = \phi \ . \tag{44}$$

Through the above relations, the differential cross section in the CM frame, written as a function of the two variables $E_{\rm cm}$ and $\Theta_{\rm cm}$, can be transformed into the corresponding quantity in the AK frame, depending on the two angular variables θ and ϕ, needed for the calculation of the transport coefficients. We can write

$$\frac{d\sigma}{d\Omega}[E_{\rm c.m.}(\theta),\Theta_{\rm cm}(\phi)] = \frac{d\sigma}{d\Omega}(\theta,\phi) \ , \tag{45}$$

with $E_{\rm c.m.}(\theta)$ and $\Theta_{\rm cm}(\phi)$ given by Eqs. (43) and (44).

In the pioneering work of Ref. [4], the scattering probability in neutron star matter was computed from Eq. (38) replacing the bare nucleon mass with an effective mass and using the nucleon-nucleon scattering cross section in free space, obtained from the measured phase shifts. This procedure accounts for the fact that both the incoming flux and the phase space available to the final state particles are affected by the presence of the medium. However, it neglects possible medium modifications of the scattering probability.

The authors of Ref. [10] improved upon the approximation of Ref. [4], using the CBF effective interaction to obtain both the effective mass and the in-medium scattering cross section of pure neutron matter within a consistent framework.

In this work, we apply the approach of Ref. [10] to the fermion hard-sphere system. The in-medium scattering probability has been computed in Born approximation using the CBF effective interaction and the definition

$$W(\theta,\phi) = \pi\left|\langle \mathbf{k}_1',\mathbf{k}_2'|v_{\rm eff}|\mathbf{k}_1,\mathbf{k}_2\rangle\right|^2 \ , \tag{46}$$

where $\mathbf{k}_i$ and $\mathbf{k}_i'$ are the initial and final momenta, respectively. The calculation of the matrix element is essentially the same as that performed in I to obtain the second order contributions to the proper self-energy. The only difference stems from the fact that, because we are considering a scattering process, here we need to average over the spins of the initial state particles. The result can be written in the form

$$\frac{1}{\nu^2}\sum_{\sigma,\sigma'}\left|\langle \mathbf{k}_1',\mathbf{k}_2'|v_{\rm eff}|\mathbf{k}_1,\mathbf{k}_2\rangle\right|^2 \tag{47}$$
$$= M^2(u) + M^2(v) - \frac{2}{\nu}M(u)M(v) \ ,$$

where $M(u)$ and $M(v)$ denote the Fourier transforms of the effective potential evaluated at

$$u = |\mathbf{k}-\mathbf{k}'| = k_F\sqrt{(1-\cos\theta)(1-\cos\phi)} \ ,$$
$$v = |\mathbf{k}+\mathbf{k}'| = k_F\sqrt{(1-\cos\theta)(1+\cos\phi)} \ . \tag{48}$$

The density dependence of the total cross section

$$\sigma_{\rm tot} = \int d\Omega \ \left(\frac{d\sigma}{d\Omega}\right), \tag{49}$$

resulting from our calculations is shown in Fig. 5 for center of mass energies $0 \le E_{\rm c.m.} \le 140$ MeV. For any given value of $E_{\rm c.m.}$, Eq. (43) implies that the Fermi momentum must satisfy the constraint $k_F > \sqrt{mE_{\rm c.m.}}$. Note that $\sigma_{\rm tot}$ is normalized to the low-energy limit obtained from the partial wave expansion of the cross section in vacuum, $\sigma_{\rm tot} = 2\pi a^2$. In Fig. 6, the same quantity is shown as a function of CM energy, with $E_{\rm c.m.} < k_F^2/m$, for different densities in the range $0.4 \le c \le 1$.

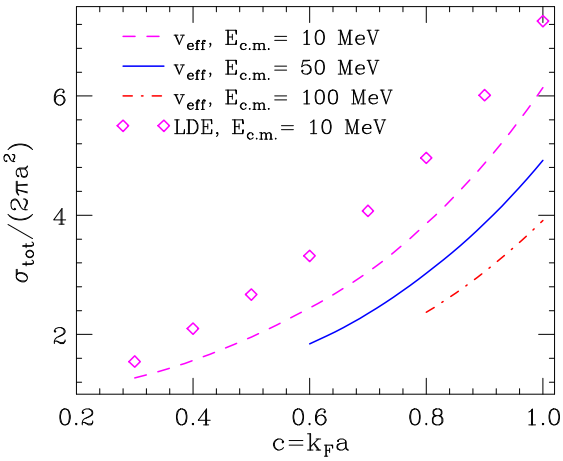

FIG. 5. (color online) c-dependence of the in-medium total cross section of the fermion hard-sphere system with ν=2—normalized to the low-energy limit in vacuum—computed using the CBF effective interaction for different values of the CM energy $E_{\rm c.m.}$. For comparison , the diamonds show the results of the low-density expansion derived in Ref. [27].

The in-medium scattering probability, defined as in Eq. (36), has been also studied within the framework of standard perturbation theory [27, 28]. The authors of Ref. [27] were able to obtain the expression of $W(\theta,\phi)$ by solving the generalised Bethe–Salpeter equation for the scattering amplitude of a dilute gas of Fermi hard

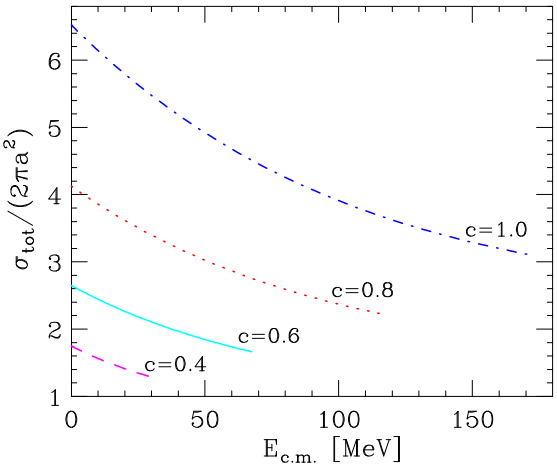

FIG. 6. (color online) $E_{\rm c.m.}$-dependence of the in-medium total cross sections of the fermion hard-sphere system with ν=2—normalized to the low-energy limit in vacuum—computed using the CBF effective interaction for different values of $c = k_F a$.

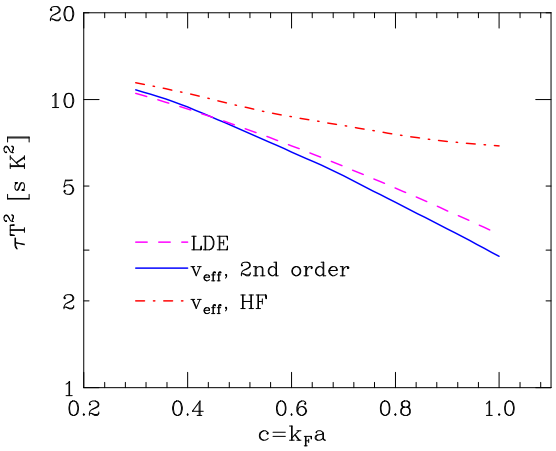

FIG. 7. (color online) c-dependence of the temperature-independent quantity τT^2, where τ is the quasiparticle lifetime of the fermion hard-sphere system of degeneracy ν=2. The dot-dash and solid lines represent the results of calculations carried out using the first and second order approximations for the effective mass, respectively, while the dashed line shows the results of the low-density expansion of Ref. [28], including terms of order up to c.

spheres including terms up to order c, corresponding to order c^2 for the scattering probability. For comparison, in Fig. 5 their results at $E_{\rm c.m.} = 10$ MeV are shown by the diamonds.

The results displayed in Figs. 5 and 6, showing that $\sigma_{\rm tot}$ increases with density, can be explained considering that the range of the effective interaction—that takes into account screening arising form dynamical correlations—is larger than the hard-sphere radius a, and grows with c (see Fig. 4 of I).

VI. TRANSPORT COEFFICIENTS

The effective mass and scattering probability discussed in the previous sections have been employed to obtain the transport coefficients of the fermion hard-sphere system with ν=2. Before analyzing the shear viscosity and thermal conductivity, in Fig. 7 we illustrate the c-dependence of the temperature-independent quantity τT^2, where τ is the quasiparticle lifetime of Eq. (7) computed using the CBF effective interaction. For comparison the prediction of the low-density expansion of Ref. [28] is also shown. Overall, the emerging pattern reflects the one observed in Fig. 4. As expected, the large corrections to the Hartree-Fock estimate of the effective mass translate into large corrections to the quasiparticle lifetime.

A. Shear viscosity and thermal conductivity

The shear viscosity coefficient of the fermion hard-sphere system of degeneracy ν=2, η, has been obtained from Eqs. (2), (4) and (8) with the effective mass and the in-medium scattering probability computed using the CBF interaction.

Figure 8 shows the c-dependence of the T-independent quantity ηT^2. The most relevant feature of the results displayed in the figure is, again, the sizable effect of second order contributions to the effective mass. As shown in Fig 4, these corrections lead to sharp increase of $m^\star$, which in turn implies a decrease of the shear viscosity coefficient η.

The T-independent quantity κT, where κ is the thermal conductivity defined by Eqs. (3), (4) and (9), is shown in Fig. 9 as a function of the dimensionless parameter c. Overall, the pattern is close to the one observed in Fig. 8.

VII. SUMMARY AND CONCLUSIONS

We have extended the analysis of the hard-sphere fermion fluid performed in I, to study the shear viscosity and thermal conductivity coefficients of the system with degeneracy ν=2, that can be regarded as a model of pure neutron matter.

In order to establish a connection between our results and those corresponding to neutron matter, in Fig. 10 we compare the momentum distribution of the fermion hard-sphere system at density corresponding to $c = 0.4$—computed with the CBF effective interaction following the procedure described in I—to those reported in Ref.[29], obtained using a quantum Monte Carlo technique. The shaded region illustrates the variation of the momentum distribution of Ref. [29] in the density

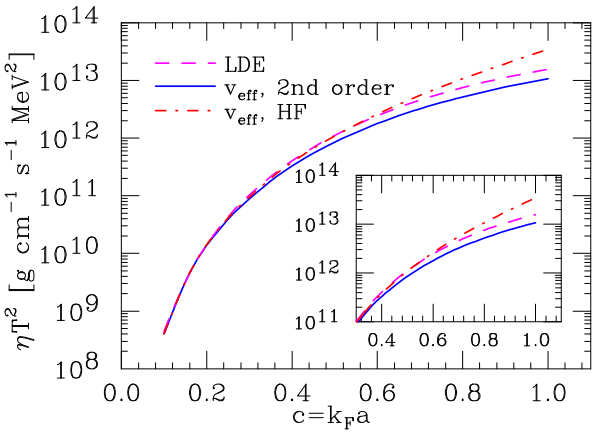

FIG. 8. (color online) c-dependence of the temperature-independent quantity ηT^2, where η is the shear viscosity coefficient of the fermion hard-sphere system of degeneracy $\nu = 2$. The dot-dash and solid lines represent the results of calculations carried out using the first and second order approximations for the effective mass, respectively, while the dashed line shows the results of the low-density expansion of Ref. [28], including terms of order up to c.

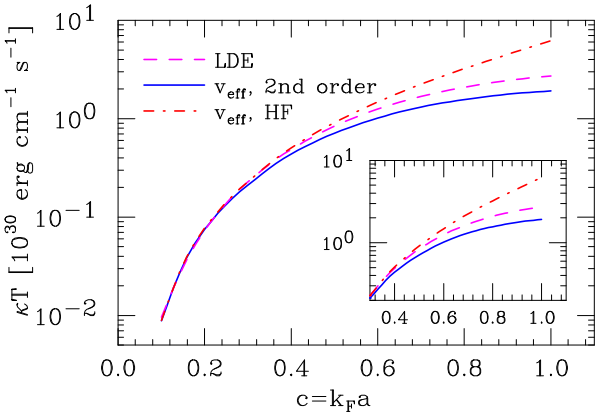

FIG. 9. (color online) c-dependence of the temperature-independent quantity κT, where κ is the thermal conductivity of the fermion hard-sphere system of degeneracy $\nu = 2$. The dot-dash and solid lines represent the results of calculations carried out using the first and second order approximations for the effective mass, respectively, while the dashed line shows the results of the low-density expansion of Ref. [28], including terms of order up to c.

range $0.08 \leq \rho \leq 0.24$ fm^{-3}. The corresponding values of the renormalisation constant are Z=0.9566 for the hard-sphere system and $0.9579 \leq Z \leq 0.9378$ for neutron matter. The appreciably higher values of $n(0)$ obtained from the Monte Carlo approach reflect the softness of the chiral neutron-neutron potential employed by the authors of Ref. [29]. The results of Fig. 10 suggest that neutrons in pure neutron matter behave similarly to hard spheres of radius $\lesssim 0.3$ fm. The same analysis for isoscalar nucleons, performed in I, leads to a radius of $\sim$0.4 fm .

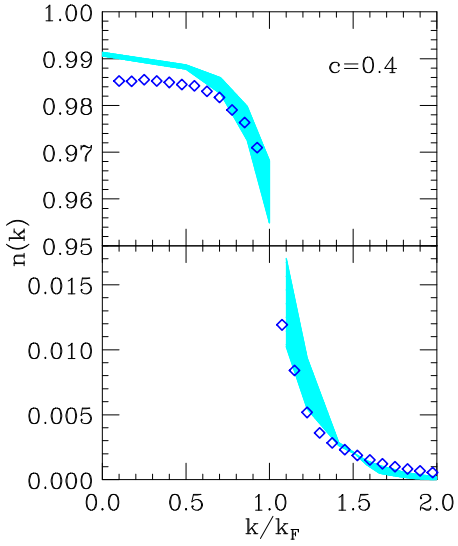

FIG. 10. (color online) Comparison between the momentum of the fermion hard-sphere system of degeneracy ν=2 at c = 0.4 (diamonds) and those reported in Ref. [29], corresponding to the density range $0.08 \leq \rho \leq 0.24$ fm^{-3} (shaded area).

The quantities needed for the calculations of the transport coefficients within the formalism developed by Abrikosov and Khalatnikov, i.e. the effective mass and in-medium scattering probability of particles on the Fermi surface, have been obtained using the approach based on the CBF effective interaction, originally derived in Refs. [10, 20]. This scheme alllows one to combine the flexibility of perturbation theory in the basis of eigenstates of the non interacting system with a realistic description of dynamical correlations in coordinate space.

Compared to the case of degeneracy ν=4, discussed in I, the derivation of the effective interaction for ν=2 involves additional difficulties arising from the presence of longer range statistical correlations. In the low-density region, corresponding to $c = k_F a < 0.5$, this problem manifests itself in the lack of a clear minimum of the FHNC energy as a function of the variational parameter describing the correlation range.

To overcome this problem and test the validity of the variational FHNC approach employed in I, the reference value of the ground-state energy, E_0, needed to determine the CBF effective interaction from Eq. (20) has been calculated using both the VMC and DMC techniques. This analysis has confirmed that, in the density region in which they are available, the FHNC results provide an accurate upper bound to the ground-state energy of the fermion hard-sphere system for both ν=2 and ν=4.

The in-medium scattering cross section, computed in Born approximation, exhibits a significant density dependence and appears to smoothly approach the low-energy

limit predicted by the partial wave expansion of the cross section in vacuum.

The real part of the proper self-energy computed at second order in the effective interaction has been employed to obtain the quasiparticle spectrum, the first derivative of which is simply related to the effective mass. As in the case ν=4, the energy-dependent second order correction significantly affects both the magnitude and the density dependence of the effective mass evaluated at $|\mathbf{k}| = k_F$.

The large second order effects on $m^\star(k_F)$ strongly impact on both the quasiparticle lifetime and the transport coefficients, leading to a suppression that monotonically increaeses with density. At density corresponding to c=$k_F a$=1, the ratio between the shear viscosity and thermal conductivity coefficients evaluated using the first and second order expressions of the effective mass turns out to be as large as ~ 3, for η, and $\sim$5 for κ. Such a big difference is likely to play an important role in astrophysical applications, and needs to be carefully investigated extending our analysis to nuclear matter.

Owing to the complexity of the nucleon-nucleon interaction and to the presence three-nucleon forces, which are known to be important at nuclear and supranuclear densities, the treatment of nuclear matter within the CBF effective interaction approach is somewhat more demanding from the computational point of view. However, it does not involve additional conceptual problems, and allows for a consistent treatment of the variety of properties—ranging from the transport coefficients to the neutrino emissivity and mean free path, to the superconducting and superfluid gaps—that concur to determine many astrophysical processes.

ACKNOWLEDGMENTS

This research is supported by the U.S. Department of Energy, Office of Science, Office of Nuclear Physics, under contract DE-AC02-06CH11357 (AL). MICINN (Spain), under grant FI-2014-54672-P and Generalitat de Catalunya, under grant 2014SGR-401 (AP), and INFN (Italy) under grant MANYBODY (AM and OB). AM gratefully acknowledges the hospitality of the Departament d'Estructura i Constituents de la Matèria of the University of Barcelona, and support from "NewCompStar", COST Action MP1304.

[1] D.G. Yakovlev, A.D. Kaminker, O.Y. Gnedin and P. Haensel, Phys. Rep. **66**, 1 (2001). 1
[2] N. Anderson and K.D. Kokkotas, Int. J. Mod. Phys. **10**, 381 (2001). 1
[3] E. Flowers and N. Itoh, Astrophys. J. **206**, 218 (1976). 1
[4] E. Flowers and N. Itoh, Astrophys. J. **230**, 847 (1979). 1, 7
[5] A.A. Abrikosov and I.M. Khalatnikov, Sov. Phys. JETP **5**, 888 (1957); Rep. Prog. Phys. **22**, 329 (1959). 1, 2
[6] G. Baym and C. Pethick, *Landau Fermi-Liquid Theory* (John Wiley & Sons, New York, 1991). 1, 2
[7] O. Benhar, A. Polls, M. Valli, and I. Vidaña, Phys. Rev. C **81**, 024305 (2010). 1
[8] H.F. Zhang, U. Lombardo, and W. Zuo, Phys. Rev. **82**, 015805 (2010).
[9] P. S. Shternin, M. Baldo, and P. Haensel, Phys. Rev. C **89**, 048801 (2014). 1
[10] O. Benhar and M. Valli, Phys. Rev. Lett. **99**, 232501 (2007). 1, 3, 6, 7, 9
[11] A. Mecca, A. Lovato, O. Benhar, and A. Polls, Phys. Rev. C **91**, 034325 (2015). 1
[12] J.P. Jeukenne, A. Lejeune, and C. Mahaux, Phys. Rep. **25**, 83 (1976). 1
[13] W. Zuo, I. Bombaci, and U. Lombardo, Phys. Rev. C **60**, 024605 (1999). 1
[14] S. Fantoni, B.L. Friman, and V.R. Pandharipande, Nucl. Phys. A **399**, 51 (1983). 1
[15] A. Rios, A. Polls, and I. Vidaña, Phys. Rev. C **79**, 025802 (2009). 1
[16] G.A. Brooker and J. Sykes, Phys. Rev. Lett. **21**, 279 (1968). 2
[17] A.L. Fetter and J.D. Walecka, *Quantum Theory of Many-Particle Systems* (McGraw-Hill, New York, 1971). 2
[18] M.H. Kalos, D. Levesque, and L. Verlet, Phys. Rev. A **9**, 2178 (1974). 2
[19] A. Fabrocini, S. Fantoni, A.Yu. Illarionov, and K.E. Schmidt, Phys. Rev. Lett. **95**, 192501 (2005). 3
[20] S. Cowell and V.R. Pandharipande, Phys. Rev. C **73**, 025801 (2006). 3, 9
[21] J.W. Clark, Prog. Part. Nucl. Phys. **2**, 89 (1979). 3, 4
[22] N. Metropolis, A.W. Rosenbluth, M.N. Rosenbluth, A.H. Teller, and E. Teller, J. Chem. Phys. **21**, 1087 (1953). 4
[23] M.H. Kalos, *Monte Carlo Methods in Quantum Problems* (Springer, Netherlands, 2012). 4
[24] R.C. Grimm and R.G Storer, J. Comp. Phys. **7**, 134 (1971). 4
[25] R.F. Bishop, Ann. Phys. **77**, 106 (1973). 4
[26] V.M. Galitskii, Sov. Phys. JETP **7**, 104 (1958). 5
[27] F. Mohling and J. C. Rainwater, J. Low Temp. Phys. **20**, 243 (1975). 7
[28] J. C. Rainwater and F. Mohling, J. Low Temp. Phys. **23**, 519 (1976). 7, 8, 9
[29] A. Roggero, A, Mukherjee, and F. Pederiva, Phys. Rev. Lett. **112**, 221103 (2014). 8, 9